

# Characteristics of the imaginary part and single-scattering albedo of urban aerosols in northern China

By JINHUAN QIU<sup>1\*</sup>, LIQUAN YANG<sup>1</sup> and XIAOYE ZHANG<sup>2</sup> <sup>1</sup>*Institute of Atmospheric Physics, Chinese Academy of Sciences, Beijing 100029, China;* <sup>2</sup>*Institute of Earth Environment, Chinese Academy of Sciences, Xian 710075, China*

(Manuscript received 17 February 2003; in final form 9 December 2003)

## ABSTRACT

An improved broadband diffuse solar radiation method for retrieval of the aerosol imaginary part (AIP) and its single-scattering albedo (SSA) is proposed. The first improvement is to determine diffuse radiation from combined pyrheliometer and pyranometer data. Secondly, available approaches to input parameters demanded for AIP retrieval are presented, including an approach to determine the aerosol extinction coefficient profile from visibility and aerosol optical depth data. This method is used to retrieve AIP and SSA from routine pyrheliometer and pyranometer observation data measured in 1993–2001 at six meteorological observatories in northern China, all located around big or medium-sized cities. As shown in the retrieval results, 9-yr mean yearly-mean AIP during 1993–2001 changed from 0.0207 to 0.0301 for the six cities, and the corresponding SSA changed from 0.851 to 0.803, with a mean value of 0.832. There are different variation trends in yearly-mean AIP and SSA during 1993–2001. At Harbin and Beijing observatories the AIP shows an increasing trend. At Shenyang and Zhengzhou observatories the AIP had an increasing trend during 1993–1995, but a decreasing trend after 1995.

Errors in the retrieved yearly-mean AIP and SSA were estimated. The main sources of AIP errors are systematic errors in the radiation measurement as well as uncertainty about the aerosol size distribution. The main error in SSA retrieval is the systematic error in the radiation data. Uncertainty about aerosol size distribution has a weak impact on SSA retrieval. It is estimated, according to sensitivity tests, that errors of yearly-mean AIP and SSA are usually within 0.0054 and 0.041 respectively.

## 1. Introduction

Atmospheric aerosols are receiving more and more attention in research into climatic forcing (Charlson et al., 1992; Kiehl and Briegleb, 1993; Penner et al., 1994; Taylor and Penner, 1994; Andronova et al., 1999; Bengtsson et al., 1999; Hignett et al., 1999; Menon et al., 2002). Aerosols are also very important in the atmospheric correction of satellite remote sensing (Kaufman et al., 1997; Gordon, 1997). Sulfate aerosols, carbonaceous aerosols and mineral dust have a substantial climatic forcing effect in a cloud-free atmosphere, comparable with the effect of greenhouse gases (Charlson et al., 1990, 1992; Penner et al., 1992, 1994; Kiehl and Briegleb, 1993). Quantitatively, however, these estimates are still quite uncertain (Kiehl and Briegleb, 1993; Taylor and Penner, 1994; Tegen et al., 1996). In particular, the lack of information about aerosol absorption is significant

(Penner et al., 1994). The same obstacle exists with regard to atmospheric correction of space-borne remote sensing, which is limiting us from obtaining accurate information from satellite data. Summarizing current research on atmospheric corrections, Kaufman et al. (1997) pointed out that the main concern is the present inadequate ability to determine aerosol absorption from space or from the ground. In addition, recent research presented by Menon et al. (2002) has shown very significant climate effects due to strongly absorbing black carbon aerosols in China and India. In the climate model of Menon et al. (2002) a key aerosol parameter, i.e. single-scattering albedo (SSA), is assumed to be 0.85 for aerosols in China.

The study of aerosol absorption or SSA requires better knowledge of aerosol properties in the real atmosphere. Of all the aerosol properties, the aerosol imaginary part (AIP) is an important parameter for determining aerosol absorption and SSA, but our knowledge of AIP is currently far from adequate. Therefore, improving the quality of this information will increase our knowledge about aerosol absorption, which is significant for estimating aerosol climate forcing.

---

\*Corresponding author.  
e-mail: jhqi@mail.iap.ac.cn

There are different ways to obtain the AIP. Laboratory measurement and remote sensing are the two main categories, and there are two kinds of remote sensing of AIP, active and passive remote sensing. One kind of passive remote sensing uses solar diffuse radiation or sky radiance information for AIP retrieval (Herman et al., 1975; King and Herman, 1978; King, 1979; Hansen, 1980; Tanaka et al., 1982; Qiu and Zhou, 1986). Herman et al. (1975) first presented a diffuse-direct method for retrieving AIP. King and Herman (1978) and King (1979) developed a method to determine ground albedo and AIP simultaneously. So far, AIP data obtained using the above methods are still very limited.

There are many routine observation data of broadband solar global/direct/diffuse radiation, measured at many meteorological stations over the world. Therefore, some efforts have been made to develop the method using the broadband solar radiation for AIP retrieval (Nakajima et al., 1996; Wei and Qiu, 1998). The method requires the input of the aerosol optical depth (AOD). In the method proposed by Nakajima et al. (1996), simultaneous sunphotometer observation is used to determine the AOD. In the method of Wei and Qiu (1998), the AOD is retrieved from pyrhe-liometer data using the method of Qiu (1998). The pyranometer used in China has a shading ring to shade direct solar radiation so as to yield the diffuse radiation, and the shaded light scattering effect is corrected. Due to the large field of view ( $10^\circ \times 180^\circ$ ) of the ring, there is often a large error in the correction. How to input the parameters demanded for AIP and SSA retrieval (including the aerosol vertical extinction profile) also remains a problem. This paper offers two main developments. First, an improved broadband solar diffuse radiation method is proposed to deal with the above two problems. Secondly, using this method, the AIP and SSA characteristics of urban aerosol in northern China during 1993–2001 are studied.

## 2. Methodology

In this section, a method for retrieval of AIP and SSA from hourly-accumulated broadband solar diffuse radiation data is presented in three parts: (1) determination of the diffuse radiation; (2) input approaches for parameters for AIP and SSA retrieval; (3) a look-up table approach for AIP and SSA retrieval.

### 2.1. Determination of solar diffuse radiation

In this paper, the solar diffuse radiation ( $S_{\text{Dif}}$ ) is determined from joint pyrhe-liometer and pyranometer data as:

$$S_{\text{Dif}} = S_{\text{Total}} - \mu_0 S_{\text{Pyr}} / (1 + R_{\text{ms}}), \quad (1)$$

where  $S_{\text{Pyr}}$  is pyrhe-liometer-detected direct solar radiation (DSR) plus the solar radiation scattered into the direct beam,  $S_{\text{Total}}$  is the total solar radiation detected by the pyranometer,  $\mu_0$  is the solar zenith angle cosine,  $R_{\text{ms}}$  is a correction factor of the scattering radiation effect on pyrhe-liometer measurement, indi-

catating the ratio of the scattering radiation to the DSR. Here  $R_{\text{ms}}$  is determined using an empirical model presented by Gueymard (1998). In the present method, the diffuse radiation error depends on the accuracy of pyrhe-liometer and pyranometer data as well as the uncertainty in  $R_{\text{ms}}$ . The radiation error and its effect on AIP and SSA retrieval will be analysed in Section 4 on error analysis.

The broadband solar diffuse radiation in the spectral range of the pyranometer response can also be determined through radiative transfer calculations as

$$S_{\text{Dif}} = \int_{\lambda_1}^{\lambda_2} S_0(\lambda) T_{\text{Dif}}(\lambda, \mu_0) d\lambda, \quad (2)$$

where  $S_0(\lambda)$  is extraterrestrial solar irradiance at the  $\lambda$ -wavelength,  $\lambda_1$  and  $\lambda_2$  are the lower and upper spectral limits of the pyranometer and  $T_{\text{Dif}}$  is the spectral diffuse transmittance. Here, calculation of  $T_{\text{Dif}}$  is required to input cloud/aerosol/molecular/gas optical parameters.

### 2.2. Input approaches for parameters for AIP and SSA retrieval

For a clear (i.e. no cloud) day, broadband solar total/direct/diffuse radiation is closely related to wavelength/height-dependent aerosol/molecular/gas optical parameters and surface albedo. If all these parameters except for AIP are known, the AIP could be retrieved through radiative transfer calculations from the broadband diffuse radiation (Nakajima et al., 1996; Wei and Qiu, 1998). A difficulty is how to input or select these parameters. Next we present approaches to inputting the main parameters demanded for AIP retrieval; these include aerosol size distribution, the real part of its refractive index, AOD and the aerosol extinction coefficient profile, molecular/gas optical depths and surface albedo.

*2.2.1. Aerosol size distribution, AOD and the real part of the aerosol refractive index.* A Junge-type aerosol size distribution (Junge, 1955) is assumed. Using this assumption and the broadband extinction method presented by Qiu (2001, 2003), the  $\lambda$ -wavelength AOD can be determined as

$$\tau_a(\lambda) = \tau_a(\lambda_E) \left( \frac{\lambda_E}{\lambda} \right)^\alpha = \tau_a(\lambda_E) \left( \frac{\lambda_E}{\lambda} \right)^{\nu^* - 2}. \quad (3)$$

In eq. (3),  $\nu^*$  is the Junge distribution parameter,  $\alpha$  is the aerosol wavelength index (Ångström exponent),  $\lambda_E$  and  $\tau_a(\lambda_E)$  are, respectively, the “effective” wavelength and the  $\lambda_E$ -wavelength AOD. Here  $\lambda_E$  and  $\tau_a(\lambda_E)$  are determined using two steps. Firstly, determine broadband AOD (BAOD) from pyrhe-liometer data (Unsworth and Monteith, 1972; Qiu, 2001). Secondly, determine the “effective” wavelength  $\lambda_E$ , at which AOD is equal to BAOD (i.e.  $\tau_a(\lambda_E) = \text{BAOD}$ ), using an approximate model from Qiu (2001, 2003).

In this paper,  $\alpha = 1$  is taken in the AIP retrievals, and the effect of its error on the retrievals is analysed latter.

The real part of the aerosol refractive index has usually a weak effect on solar diffuse radiation and shows a relatively small variation in the wavelength range of 0.3–2  $\mu\text{m}$ ; a value of 1.5 is taken for it.

2.2.2. *Aerosol extinction coefficient profile.* The aerosol extinction coefficient ( $\sigma_a$ ) profile is assumed as

$$\sigma_a(z, \lambda) = \sigma_a(0, \lambda) \exp(-z/z_a), \quad (4)$$

where  $\sigma_a(0, \lambda)$  is the aerosol extinction coefficient at the surface level and  $z_a$  indicates the decreasing slope of the aerosol extinction coefficient. It can be derived from eq. (4) that

$$\tau_a(\lambda) = \sigma_a(0, \lambda) z_a. \quad (5)$$

There is a relationship  $\sigma_a(0, \lambda)$  at  $\lambda = 0.55 \mu\text{m}$  with the surface visibility ( $V$ ), given by

$$V = 3.912/\sigma_a(0, 0.55 \mu\text{m}). \quad (6)$$

Then, using the AOD retrieved from pyrhelimeter data, two parameters  $\sigma_a(0, \lambda)$  and  $z_a$  in eq. (4) can be determined as

$$\sigma_a(0, \lambda) = \frac{3.912}{V} \left( \frac{0.55}{\lambda} \right)^\alpha. \quad (7)$$

$$\begin{aligned} z_a &= \tau_a(\lambda)/\sigma_a(0, \lambda) \\ &= \tau_a(\lambda) \frac{V}{3.912} \left( \frac{\lambda}{0.55} \right)^\alpha. \end{aligned} \quad (8)$$

Under the assumption of height-independent aerosol size distribution and refractive index,  $z_a$  is also wavelength-independent. In this paper, monthly-mean  $z_a$ , derived from AOD and visibility data according to eq. (8), is used in practical AIP retrieval.

2.2.3. *Molecular/gas optical depths.* The molecular scattering optical depth  $\tau_{\text{ms}}(0.55 \mu\text{m}, z_0)$  for a wavelength of 0.55  $\mu\text{m}$  and a sea level height ( $z_0$ ) is taken from MODTRAN (Berk et al., 1996), and  $\tau_{\text{ms}}(\lambda, z_0)$  for other wavelengths is given by

$$\tau_{\text{ms}}(\lambda, z_0) = \tau_{\text{ms}}(0.55 \mu\text{m}, z_0) \left( \frac{\lambda}{0.55} \right)^{-4}, \quad (9)$$

The absorbing optical depths of ozone and water vapour are also calculated using MODTRAN. The calculation needs to input the vertical amount of ozone and water vapour. Over the Beijing site, the total amounts of ozone are selected from the monthly-mean Dobson observation data. Over the other sites, the amounts of ozone from Total Ozone Mapping Spectrometer (TOMS) data are used. The amount of water vapour ( $U$ ) is determined from the surface water vapour pressure, using the following empirical expression presented by Yang and Qiu (2002):

$$U = a_0 + a_1 e + a_2 e^2. \quad (10)$$

In this expression the three empirical coefficients  $a_0$ ,  $a_1$  and  $a_2$  are site-dependent.

2.2.4. *Surface albedo.* Surface albedo has a weaker effect on solar diffuse radiation than AIP. Monthly-mean Moderate Resolution Imaging Spectroradiometer (MODIS) albedo products with a resolution of 0.25° are used in AIP retrieval.

### 2.3. Look-up table approach for AIP and SSA retrieval

In order to save computing time in AIP retrieval, a look-up table approach is used, and the DISORT code (Stamnes et al., 1988) is applied to build the broadband solar diffuse radiation table. In the table the input parameters are selected as:

- (1) surface albedo: 0.08, 0.15, 0.25 and 0.35;
- (2) 1  $\mu\text{m}$ -wavelength AOD ( $\beta$ ): 0.1, 0.25, 0.4, 0.7, 1.0, 1.5, 2.0 and 3.0;
- (3) solar zenith angle cosine: 1.0, 0.95, 0.9, 0.8, 0.6, 0.5, 0.4 and 0.3;
- (4) column H<sub>2</sub>O amount (cm): 0.1, 0.5, 1.0, 2.0, 3.0, 5.0 and 7.0;
- (5) total amount of ozone (cm): 0.25, 0.35 and 0.45;
- (6) sea level height (km): 0.0, 0.3, 0.6, 1.0, 1.5 and 2.0;
- (7) AIP: 0, 0.005, 0.01, 0.015, 0.02, 0.03, 0.04, 0.05, 0.06 and 0.08;
- (8) Junge distribution parameter  $\nu^*$ : 2.0, 2.5, 3.0, 3.5 and 4.0.
- (9) aerosol extinction profile parameter  $z_a$ : 1.2, 2.0, 3.0 and 4.0.

For the MODTRAN rural aerosol model with a surface visibility of 23 km the value  $z_a$  is equal to 2.089, and for the urban aerosols over the six observatories studied in this paper the monthly-mean  $z_a$  changes between 1.2 and 4.0. So an  $z_a$  range from 1.2 to 4.0 is considered. The radiation table also lists the 1  $\mu\text{m}$ -wavelength SSAs for the above-mentioned five Junge size distributions and 10 AIP values. Using the table, AIP and SSA are simultaneously retrieved from joint pyrhelimeter and pyranometer data. These data are hourly-exposed radiations, and a mean solar zenith angle cosine is taken for the AIP retrievals, given by:

$$\mu_{\text{Mean}} = (\mu_{00} + \mu_{60})/2. \quad (11)$$

In eq. (11),  $\mu_{00}$  and  $\mu_{60}$  are the solar zenith angle cosines at the beginning and the sixtieth minute during 1 h.

## 3. Characteristics of AIP and SSA of urban aerosols around six cities

The above-mentioned method is used in the retrieval of AIP and SSA from hourly-exposed pyrhelimeter and pyranometer data measured at six meteorological observatories during 1993–2001. As shown in Fig. 1, the observatories are located around the six cities of Harbin, Shenyang, Beijing, Urumqi, Lanzhou and Zhengzhou in northern China. Table 1 shows the population in 1998 and land use situation in these cities (Luo et al., 2001) as well as yearly-mean cloud fraction and AOD in 2000. These

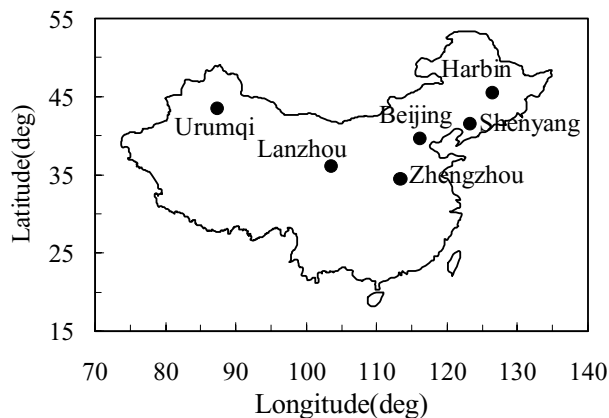


Fig 1. Map showing location of six meteorological observatories.

cities are all industrial, and the yearly-mean cloud fraction there ranged from 41.4% (Beijing) to 58.4% (Lanzhou) in 2000. According to some measurements presented by Winchester et al. (1981), Wang et al. (2002) and Zhang et al. (2003), the three main types of aerosol in northern China are sulfate aerosols, mineral dust and carbonaceous aerosols.

The AIP and SSA retrievals require input of surface water vapour pressure, visibility and cloud fraction data. There are three day-time records of these data at meteorological observatories in China, made at 08:00, 14:00 and 20:00 local time (LT) respectively. Their values at other times are obtained from the three records through linear interpolation. The cloud fraction ( $C_f$ ) is used to select radiation data for AIP retrieval. Only radiation data without any cloud cover ( $C_f = 0$ ) and during 08:00–09:00 or 13:00–15:00 are selected in order to eliminate the cloud effect. According to this constraint, if  $C_f = 0$  at 08:00 and 14:00 but  $C_f > 0$  at 20:00, only two sets of radiation data during 08:00–09:00 and 13:00–14:00 are selected for AIP retrieval. If  $C_f = 0$  at 08:00 but  $C_f > 0$  at 14:00 and 20:00, no radiation data are selected.

There is usually a larger error in pyranometer measurement when the solar zenith angle  $\theta_0$  is beyond  $75^\circ$ , due to the cosine response characteristics of the instrument. Therefore, another constraint upon radiation data selection is  $\theta_0 < 65^\circ$ . In addition, when AOD increases, or  $\mu_0$  decreases, the diffuse radiation

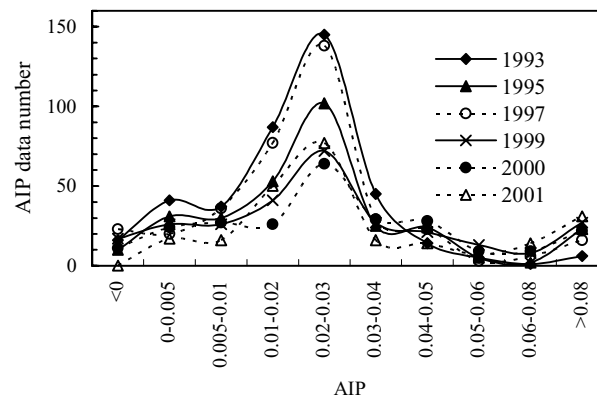


Fig 2. Numbers of AIP data in different AIP ranges for Beijing during 1993–2000.

becomes more sensitive to the variation in AIP (Herman et al., 1975; Wei and Qiu, 1998). The stronger the sensitivity, the higher the accuracy of the retrieved AIP. Based on this fact, the third constraint upon radiation data selection is that the ratio of the  $1 \mu\text{m}$ -wavelength AOD ( $\beta$ ) to  $\mu_0$  is larger than 0.4 ( $\beta/\mu_0 > 0.4$ ).

Using the retrieved AIP and the assumed aerosol wavelength index ( $\alpha = 1.0$ ), SSA at the  $1 \mu\text{m}$  wavelength is simultaneously determined. Next, AIP and SSA characteristics over the six sites are analysed according to the retrieval results shown as in Figs. 2–6.

Figure 2 shows numbers of AIP data in different AIP solution ranges for the Beijing site during 1993–2001. It can be seen that most AIP data are in the range of 0.01–0.03. In addition, there are more than 160 sets of AIP data for every year. When the calculated diffuse radiation corresponding to  $k = 0$  (AIP) is larger than the measured radiation, the AIP solution is regarded as “negative (<0)”. Data with an unreasonably negative AIP solution comprise fewer than 8% of the total. The larger AIP solution may be caused by errors in the input parameters or horizontal inhomogeneity of the atmosphere, and so AIP of  $>0.08$  is also not used in the latter AIP estimation.

Figures 3 and 4 illustrate total yearly/seasonal-mean AIP and SSA during 1993–2001 for the six cities. Here December, January and February are regarded as the winter, March, April

Table 1. Features of six cities in China

City	Population (1998)	Land use	AOD (2000)	Per cent cloud fraction
Harbin	2 991 608	Industry	0.344	49.0
Shenyang	4 799 851	Industry	0.389	50.8
Beijing	8 130 686	Industry	0.535	41.4
Urumqi	1 391 896	Industry	0.451	45.7
Lanzhou	1 749 752	Industry	0.522	58.4
Zhengzhou	2 039 286	Industry	0.816	58.3

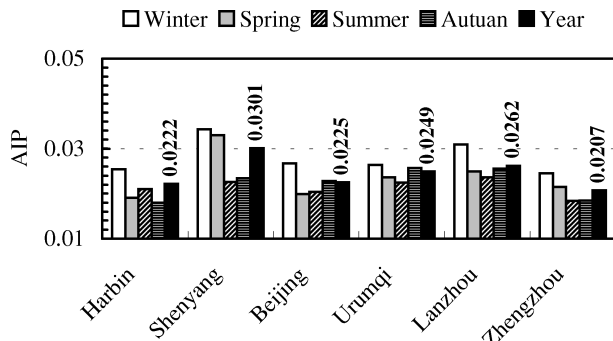


Fig 3. Total yearly/seasonal-mean AIPs during 1993–2001.

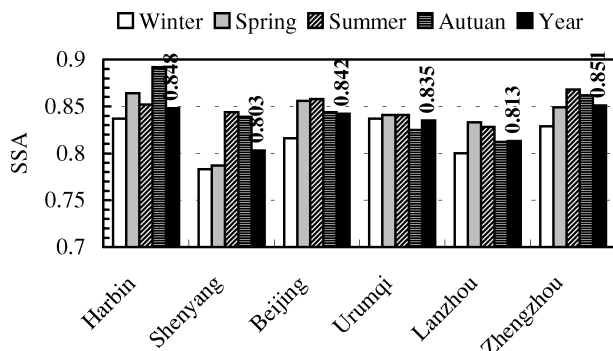


Fig 4. Total yearly/seasonal-mean SSAs during 1993–2001.

and May are the spring, June, July and August are the summer and September, October and November are the autumn. First, we determine yearly/seasonal-mean AIP and SSA for each year during 1993–2001; then the nine mean values are further averaged to yield the total yearly/seasonal-mean AIP and SSA. It can be seen from Figs. 3 and 4 that:

(1) The yearly-mean AIP (digits in Fig. 3) changes from 0.0207 (Zhengzhou) to 0.0301 (Shenyang), and the corresponding SSA (digits in Fig. 4) from 0.851 to 0.803 with a mean value of 0.832. Shenyang is the capital of Liaoning province, a centre for heavy industry in China, where many heavy-industrial factories are situated, including large steel factories and power plants. This fact is treated as a significant reason for the largest AIP being there.

(2) For the continental aerosol model presented by Lenoble (1985), volume percentages of water-soluble, dust-like and soot aerosols are 29%, 70% and 1% respectively. For the continental aerosol model the SSA from the Mie scattering calculation is 0.875. For an urban industrial aerosol in the height range 0–2 km the respective percentages are 61%, 17% and 22% and the corresponding SSA is 0.67. The mean SSA value for the six cities in this study is 0.832, being between the two SSA values of 0.875 and 0.67.

(3) The AIP and SSA have an evident seasonal variation. In winter, the AIP is larger, especially for Shenyang, and the corresponding SSA is smaller. November to the following February

is the period in northern China when, increasingly, coal-burning for heating purposes is mainly responsible for the larger AIP. In the summer, the AIP is usually smaller, partly due to the higher humidity.

As shown in Fig. 5, there are different variation trends in yearly mean AIP and SSA during 1993–2001. Over the Harbin site (Fig. 5a), the AIP (respectively SSA) has an evidently increasing (respectively decreasing) trend during 1993–2001. The SSA decreases from 0.882 in 1993 to 0.798 in 2001. Over the Shenyang site (Fig. 5b), there is a minimum value of AIP in 1995, and from 1995 to 1998 the AIP has a decreasing trend. Over Beijing site (Fig. 5c), there is a minimum value of AIP in 1996, and after 1996 there is evidently an increasing trend in AIP. As shown Fig.5d, the AIP over the Urumqi site changes between 0.023 and 0.027 during 1993–2001, showing a relatively small difference. Over the Lanzhou site (Fig. 5e) before 1998 the AIP has an increasing trend, but after 1999 it has a decreasing trend. Over the Zhengzhou site (Fig. 5f), the AIP has an evidently decreasing trend after 1997.

The AIP obtained using the present method indicates a mean imaginary part characteristic of all aerosol compositions in the total atmospheric column. The mean AIP depends on the constitution and optical parameters (including their size distributions and imaginary parts) of these compositions. If the concentration of strongly absorbing carbonaceous aerosol increases more quickly (or decreases more slowly) than the weakly absorbing aerosol, the proportion of carbonaceous aerosol would increase, and thus the AIP would become larger if there is no change in size distribution and AIP of all aerosol components. According to measurement results presented by Wang et al. (2002), the concentration of black carbon aerosol in Beijing in late autumn has an increasing trend from 1996 to 1999 and a decreasing trend from 1999 to 2001. As shown in Fig. 6, there is an evidently decreasing trend of the total column AOD in Beijing from 1997 to 2001, particularly evident after 1999. As a result, there may be an increase in the proportion of black carbon aerosol during 1996–2001, causing a trend of increasing AIP (see Fig. 5c) in the period. Owing to a lack of true aerosol composition measurements, further explanations of above-mentioned variation characteristics of AIP and SSA remain a problem.

#### 4. Error analysis

The main errors in AIP and SSA retrieval by the present method include:

- (1) error in the radiation measurement;
- (2) aerosol size distribution uncertainty;
- (3) uncertainty of the surface albedo;
- (4) errors in the amounts of column water vapour and ozone;
- (5) error of the aerosol optical depth;
- (6) the cloud effect.

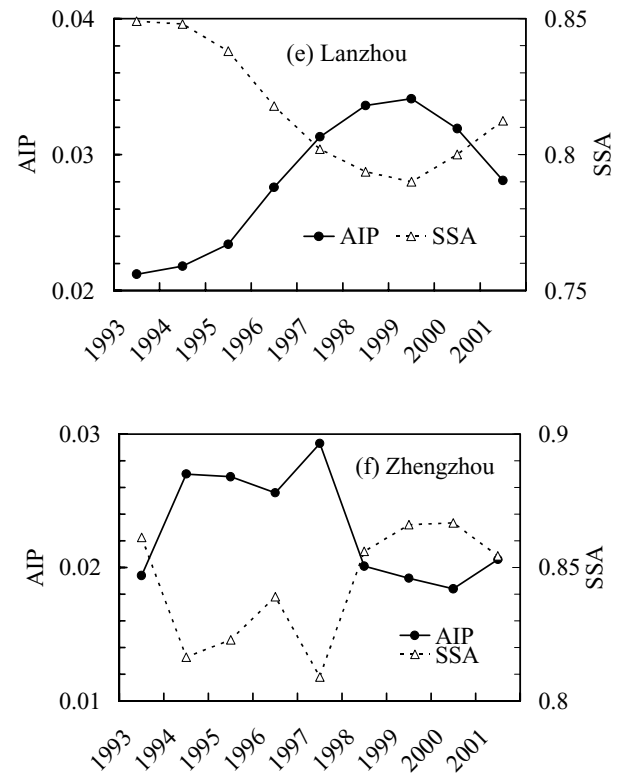
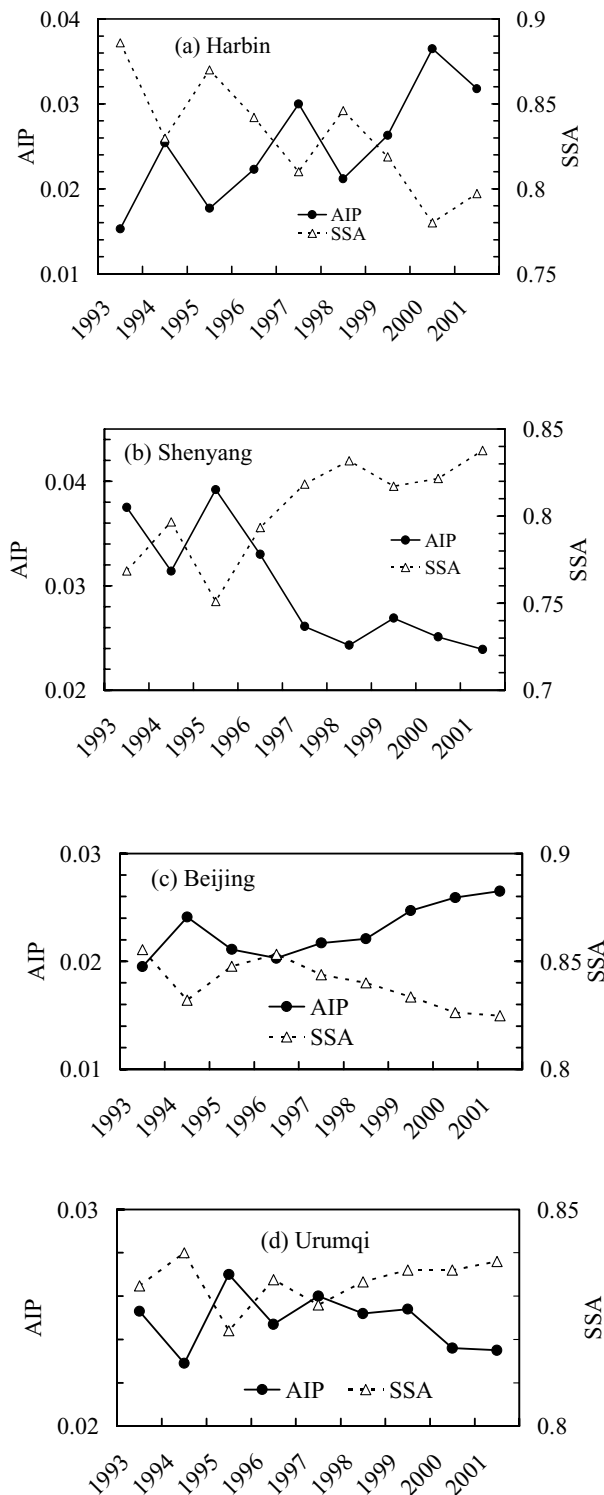


Fig 5. Continued.

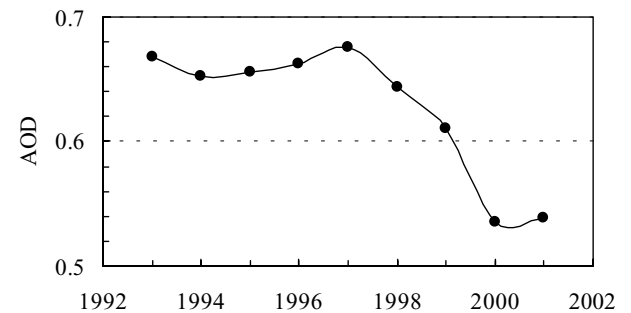


Fig 6. Yearly-mean AOD retrieved from pyrheliometer data for Beijing during 1993–2001.

Fig 5. Variation characteristics of yearly-mean AIP and SSA during 1993–2001 for Harbin (a), Shenyang (b), Beijing (c), Urumqi (d), Lanzhou (e) and Zhengzhou (f).

Now, the effects of the first five error factors on AIP and SSA retrieval are analysed according to retrieval simulations, and the cloud effect is qualitatively analysed. In the simulations, it is assumed that there are no errors in the following input parameters: radiative data, MODIS surface albedo products, AOD, amount of column water vapour and ozone, and Junge aerosol size distribution with  $\nu^* = 3$ . The AIP difference caused by modifying these parameters is treated as the error in AIP retrieval. The modification for all input parameters is defined as:

$$y = (1 + \delta_{\text{sys}} + \delta_{\text{ran}})y_0, \tag{12}$$

where  $y_0$  and  $y$  are original and modified input parameters,  $\delta_{\text{sys}}$  and  $\delta_{\text{ran}}$  indicate the systematic and random errors in the input

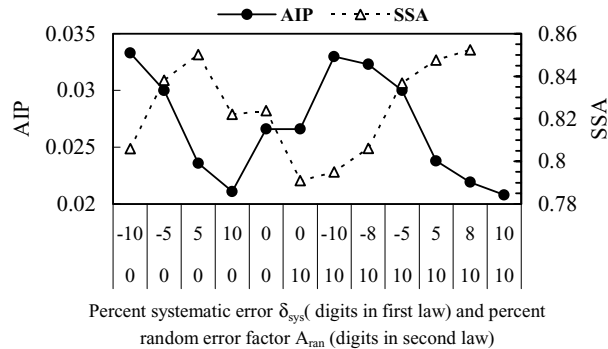


Fig 7. Effect of error in the radiation data on yearly-mean AIP and SSA retrievals for Beijing in 2000.

parameter  $y_0$ , respectively. The random error is given by:

$$\delta_{\text{ran}} = (1 - 2x)A_{\text{ran}}, \quad (13)$$

where  $x$  is taken from computer random numbers ranging between 0 and 1, and  $A_{\text{ran}}$  is called the modifying factor of the random error. If  $A_{\text{ran}}$  is equal to 0.1 (10%), the random error changes between  $-10\%$  and  $10\%$ . The relative systematic error  $\delta_{\text{sys}}$ , being equal to a positive or negative constant, is assumed.

Next, effects of the above-mentioned six error factors on yearly-mean AIP and SSA estimations for Beijing site during 2000 are analysed.

(1) **Effect of error in the radiation data.** As shown in eq. (1), the error in the determination of diffuse radiation mainly depends on the accuracy of pyrheliometer and pyranometer data. The radiation data used in this study are all from first-class meteorological observatories in China, in which the pyranometers and pyrheliometers are calibrated once every 2 yr by comparing with international standard instruments. The error of the pyranometer measurements for the solar zenith angle of  $\theta_0 < 70^\circ$  is usually within 5%, and the pyrheliometer accuracy is usually better than 2%. Based on the accuracy, it is estimated according to radiation calculations that the error in the diffuse radiation determination is within  $\pm 13\%$  in the condition of  $\beta/\mu_0 > 0.4$  (here  $\beta$  is the  $1 \mu\text{m}$ -wavelength AOD).

Figure 7 shows effect of systematic and random errors in the diffuse radiation determination on yearly-mean AIP and SSA estimations. Here the radiation error inputs are:  $\delta_{\text{sys}} = -10\%$ ,  $-8\%$ ,  $-5\%$  and  $5\%$ ,  $8\%$  and  $10\%$ ;  $A_{\text{ran}} = 10\%$ . As shown in Fig. 7, the random radiation error has a weak effect on yearly-mean AIP and SSA. The AIP and SSA errors caused by random radiation error within  $\pm 10\%$  are only 0.0005 and 0.004 respectively. But the systematic radiation error has relatively strong effect. As the error is 5% or  $-5\%$ , errors of yearly-mean AIP and SSA are within 0.0037 and 0.033. When systematic and random errors in the diffuse radiation data are 10% (or  $-10\%$ ) and within  $\pm 10\%$ , errors of the yearly-mean AIP and SSA are within 0.0054 and 0.041 respectively.

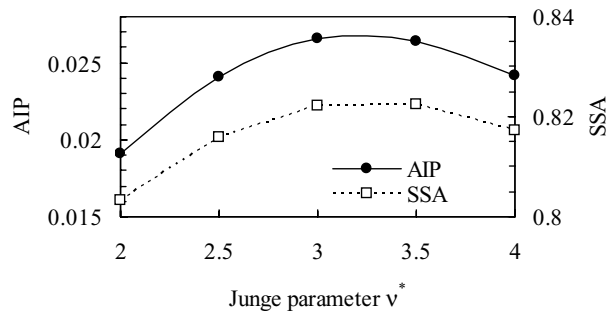


Fig 8. Effect of uncertainty in the aerosol size distribution on yearly mean AIP and SSA retrievals for Beijing in 2000.

Table 2. Errors ( $\Delta\kappa/\Delta\omega_a$ ) in yearly-mean AIP and SSA for the Beijing site in 2000, caused by errors in the  $\text{H}_2\text{O}$  amount ( $\delta_{\text{sys}}/A_{\text{ran}}$ )

$\delta_{\text{sys}}/A_{\text{ran}}$	$-10\%/0$	$10\%/0$	$10\%/10\%$
$\Delta\kappa/\Delta\omega_a$	$0.0004/-0.002$	$-0.0004/0.003$	$-0.0004/0.003$

According to retrieval calculations, the scattering correction factor  $R_{\text{ms}}$  is usually within 5%, its uncertainty has a relatively weaker effect on the determination of diffuse radiation and then AIP retrieval. If the  $R_{\text{ms}}$  error is 20%, the corresponding yearly-mean AIP error is 0.0008 for the Beijing site in 2000.

(2) **Effect of aerosol size distribution uncertainty.** Figure 8 shows effects of an aerosol size distribution uncertainty on AIP and SSA retrieval. The typical value of the Junge distribution parameter  $\nu^*$  is 3.0 for urban aerosols (Junge, 1955). The measurements presented by Qiu et al. (1988) also showed that the typical  $\nu^*$  over the Beijing area was close to 3.0. When there is a  $\pm 0.5$  error in the Junge distribution parameter  $\nu^*$ , deviations of the yearly -mean AIP and SSA (compared with the result of  $\nu^* = 3$ ) are within 0.0026 and 0.006 (see Fig. 8) respectively. The effect of the size distribution uncertainty on the SSA solution is weaker.

(3) **Effects of errors in column water vapour and ozone amounts.** The column water vapour ( $\text{H}_2\text{O}$ ) amount is derived from the surface water vapour pressure, using an empirical expression presented by Yang and Qiu (2002). The expression error is usually within 20% for most areas in China. As shown in Table 2, if the error (including a 10% systematic error) in the  $\text{H}_2\text{O}$  amount is within 20%, errors in yearly-mean AIP and SSA are 0.0004 and 0.003 respectively, implying a very satisfactory accuracy.

The effect of error in the amount of ozone on AIP and SSA is very weak. If the ozone error is within 20%, the AIP and SSA errors can be within 0.0001 and 0.002 respectively.

(4) **Effect of error in aerosol optical depth.** Table 3 shows errors ( $\Delta\kappa/\Delta\omega_a$ ) of yearly-mean AIP and SSA caused by an AOD uncertainty. The error of AOD retrieved from

Table 3. Errors ( $\Delta\kappa/\Delta\omega_a$ ) of yearly-mean AIP and SSA for the Beijing site in 2000, caused by AOD errors ( $\delta_{\text{sys}}/A_{\text{ran}}$ )

$\delta_{\text{sys}}/A_{\text{ran}}$	-10%/0	10%/0	10%/10%
$\Delta\kappa/\Delta\omega_a$	-0.0013/0.008	0.0013/-0.006	0.0013/-0.006

pyrheliometer data is usually less than 10%, and its mean value has a higher accuracy (Qiu, 1998). As shown in Table 3, when systematic and random errors of the AOD are 10% and within  $\pm 10\%$ , errors of yearly-mean AIP and SSA can be within 0.0012 and 0.005 respectively.

(5) **Effect of surface albedo uncertainty.** According to retrieval simulations, if there is a 20% error of the MODIS surface albedo products, deviations of the yearly-mean AIP and SSA for the Beijing site in 2000 are, respectively, within 0.0008 and 0.0039.

(6) **Cloud effect.** As mentioned above, the used cloud fraction ( $C_f$ ) is determined from the three day-time records through linear interpolation. Owing to temporal and spatial variation of cloud cover, even the determined  $C_f$  is equal to zero; there is also some possibility of the presence of (especially broken) cloud cover during the period beyond the recording time. The presence of broken cloud cover ordinarily increases the diffuse short-wave radiation because of the increase of scattering (compared to molecular-aerosol scattering) by cloud (Long and Ackerman, 2000). The radiation increase would result in an underestimated (even negative) AIP. In northern China a longer period without any cloud cover was often observed. For example, during 7 days from 25 to 31 January 2000, cloud cover records in Beijing were all zero. Based on this fact, the urban aerosol around six cities in northern China is studied in this paper. There may be a few retrievals confronted with a stronger cloud effect, which generally result in an underestimated (even negative) AIP solution. However, as far as the yearly/seasonal-mean AIP/SSA estimations from many AIP/SSA solutions are concerned, the effect can be relatively small.

Summarizing above analysis, it can be concluded that the errors of the present yearly/seasonal-mean AIP/SSA estimations are caused mainly by systematic error in the radiation data.

## 5. Summary

An improved broadband diffuse radiation method for AIP retrieval is proposed. The first improvement is to determine diffuse radiation from combined pyrheliometer and pyranometer data in order to avoid shading ring correction. Secondly, available approaches to input parameters demanded for AIP and SSA retrieval are presented.

This broadband diffuse radiation method is used in retrieving AIP and SSA from routine pyrheliometer and pyranometer observations around six cities in northern China during 1993–2001.

The main conclusions from the retrieval results are summarized as follows:

(1) The total yearly-mean AIPs during 1993–2001 change from 0.0207 to 0.0301 for the six cities, and the corresponding SSA from 0.851 to 0.803, with a mean value of 0.832. The SSA mean is close to the SSA selection (0.85) used in the climate simulation of (Menon et al., 2002).

(2) The AIP is larger during the winter (period for using heating in northern China) for all sites, especially for the Shenyang site, owing to the increase in coal burning. The AIP during summer is smaller for all sites except for Harbin (it is larger for Harbin).

(3) There are different variation trends in AIP and SSA. Over Harbin site the AIP (respectively SSA) has an evidently increasing (respectively decreasing) trend during 1993–2001. Over the Beijing site, after 1996 there is an evidently increasing trend in AIP. Over the Zhengzhou site, the AIP has an increasing trend during 1993–1995 but evidently decreasing after 1997.

It is emphasized that there are three constraints to radiation data used in AIP retrieval in order to improve the accuracy of the AIP. These constraints are: (1) the cloud fraction ( $C_f$ ) is equal to zero; (2) the solar zenith angle is less than  $65^\circ$ ; (3) the ratio of the  $1\ \mu\text{m}$ -wavelength AOD to the solar zenith angle cosine is larger than 0.4.

An estimation of the error of yearly-mean AIP and SSA is made. The main sources resulting in AIP error are systematic error in the radiation measurement and uncertainty of aerosol size distribution, but especially the first one. The main error factors for SSA retrieval are the systematic error in the radiation measurement. Uncertainty of aerosol size distribution has a weak effect. It is estimated that the systematic error in the determination of diffuse radiation is usually within 10%. Under the error limits, it is estimated that errors of yearly/season mean AIP and SSA are usually within 0.0054 and 0.041.

Owing to a lack of true aerosol composition measurements, further explanation of the variation characteristics of AIP and SSA remains a problem.

## 6. Acknowledgements

This research is supported by National Natural Science Foundation of China (Grant No. 40205006 and No. 40175009) and the National Development Project of Fundamental Research (G1999045700), and the surface albedo used is taken from MODIS products.

## References

- Andronova, N. G., Rozanov, F. Y., Schlesinger, M. E. and Stenchikov, G. L. 1999. Radiative forcing by volcanic aerosols from 1850 to 1994. *J. Geophys. Res.* **104**(D14), 16807–16816.
- Bengtsson, L., Roeckner, E. and Stendel, M. 1999. Why is the global warming proceeding much slower than expected. *J. Geophys. Res.* **104**(D4), 3865–3878.

- Berk, A., Bernstein, L. S. and Robertson, D. C. 1996. *MODTRAN: A moderate resolution model for LOWTRAN 7*, GL-TR-89-0122 (1989), updated and commercialized by Ontar Corporation, 9 Village Way, North Andover, MA 01845.
- Charles, N. L. and Thomas, P. A. 2000. Identification of clear skies from broadband pyranometer measurements and calculation of downwelling shortwave cloud effects. *J. Geophys. Res.* **105**(D12), 15 609–15 626.
- Charlson, R. J., Schwartz, S. E., Hales, J. M., Cess, R. D., Coakley, J. A., Hansen, J. E. Jr. and Hofmann, D. J. 1992. Climate forcing by anthropogenic aerosols. *Science* **255**, 423–429.
- Charlson, R. J., Langner, J. and Rodhe, H. 1990. Sulphate aerosol and climate. *Nature* **348**, 22–25.
- Gueymard, C. 1998. Turbidity determination from broadband irradiance measurements: a detailed multicoefficient approach. *J. Appl. Meteorol.* **37**, 414–435.
- Gordon, H. R. 1997. Atmospheric correction of ocean color imagery in the Earth observing system era. *J. Geophys. Res.* **102**(D14), 17081–17106.
- Hansen, M. Z. 1980. Atmospheric particulate analysis using angular light scattering. *Appl. Opt.* **19**, 3441–3448.
- Herman, B. M., Browning, S. R. and De Luisi, J. J. 1975. Determination of the effective imaginary term of the complex refractive index of atmospheric dust by remote sensing: the diffuse-direct radiation method. *J. Atmos. Sci.* **32**, 918–925.
- Hignett, P., Taylor, J. P., Francis, P. N. and Glew, M. D. 1999. Comparison of observed and modeled direct aerosol forcing during TARFOX. *J. Geophys. Res.* **104**(D2), 2279–2287.
- Junge, C. E. 1955. The size distribution and aging of natural aerosols as determined from electrical and optical data on the atmosphere. *J. Meteorol.* **12**, 13–25.
- Kaufman, Y. J., Tanre, D., Gordon, H. R., Nakajima, T., Lenoble, J., Frouin, R., Grassl, H., Herman, B. M., King, M. D. and Teillet, P. M. 1997. Passive remote sensing of tropospheric aerosol and atmospheric correction for the aerosol effect. *J. Geophys. Res.* **102**, 16815–16830.
- Kiehl, J. T. and Briegleb, B. P. 1993. The radiative role of sulfate aerosols and greenhouse gases in climate forcing. *Science* **260**, 311–314.
- King, M. D. 1979. Determination of the ground albedo and the index of absorption of atmospheric particulates by remote sensing. Part two: Application. *J. Atmos. Sci.* **36**, 1072–1083.
- King, M. D. and Herman, B. M. 1978. Determination of the ground albedo and the index of absorption of atmospheric particulates by remote sensing. Part one: Theory. *J. Atmos. Sci.* **36**, 163–173.
- Lenoble, J. 1985. *Radiative Transfer in Scattering and Absorbing Atmospheres: Standard Computational Procedures*. A. Deepak Publishing, Hampton, VA.
- Long, C. N. and Ackerman, T. P. 2000. Identification of clear skies from broadband pyrliometer measurements and calculation of downwelling shortwave cloud effects. *J. Geophys. Res.* **105**, D12, 15609–15626.
- Luo, Y., Lu, D., Zhou, X., Li, W., and He, Q. 2001. Characteristics of the spatial distribution and yearly variation of aerosol optical depth over China in the last 30 years. *J. Geophys. Res.* **106**, D13, 14501–14513.
- Menon, S., Hansen, J., Nazarenko, L. and Luo, Y. 2002. Climate effects of black carbon aerosols in China and India, *Science* **297**, 2250–2253.
- Nakajima, T., Hayasaka, T., Higrashi, A., Hashida, G., Moharram-Nejad, N., Yahya, N. and Hamzeh, V. 1996. Aerosol optical properties in the Iranian region obtained by ground-based solar radiation measurements in the summer of 1991. *J. Appl. Meteorol.* **35**, 1265–1278.
- Penner, J. E., Dickinson, R. and O'Neill, C. 1992. Effects of aerosol from biomass burning on the global radiation budget. *Science* **256**, 1432–1434.
- Penner, J. E., Charlson, R. J., Hales, J. M., Laulainen, N. S., Leifer, R., Novakov, T., Ogren, J., Radke, L. F., Schwartz, S. E. and Travis, L. 1994. Quantifying and minimizing uncertainty of climate forcing by anthropogenic aerosols. *Bull. Am. Meteorol. Soc.* **75**, 375–400.
- Qiu, J. 1998. A method to determine atmospheric aerosol optical depth using total direct solar radiation. *J. Atmos. Sci.* **55**, 734–758.
- Qiu, J. 2001. Broadband extinction method to determine atmospheric aerosol optical properties, *Tellus* **53B**, 72–82.
- Qiu, J. 2003. Broadband extinction method to determine aerosol optical depth from accumulated solar direct radiation, *J. Appl. Meteorol.* **42**, 1611–1625.
- Qiu, J. and Sun, J. 1994. Optically remote sensing of the dust storm and the analysis. *Chinese J. Atmos. Sci.* **18**, 1–10.
- Qiu, J. and Yang, L. 2000. Variation characteristics of atmospheric aerosol optical depths and visibility in North China during 1980–1994. *Atmos. Environ.* **34**, 601–607.
- Qiu, J. and Zhou, X. 1986. Simultaneous determination of the aerosol size distribution, refractive index, and surface albedo from radiance? Part I: Theory. *Adv. Atmos. Sci.* **3**, 162–171.
- Qiu, J., Sun, J., Xia, Q. and Zhang, J. 1988. Remote sensing and analysis of aerosol optical properties in Beijing. *Acta Meteorol. Sinica* **46**, 49–58.
- Stamnes, K., Tsay, S. C., Wiscombe, W. J. and Jayaweera, K. 1988. Numerically stable algorithm for discrete ordinate method radiative transfer in multiple scattering and emitting layered media. *Appl. Opt.* **27**, 2502–2509.
- Tanaka, M., Takamura, T. and Nakajima, T. 1982. Refractive index and size distribution of aerosols as estimated from light scattering measurements. *J. Clim. Appl. Meteorol.* **2**, 1253–1261.
- Taylor, K. E. and Penner, J. E. 1994. Response of the climate system to atmospheric aerosols and greenhouse gases. *Nature* **369**, 734–737.
- Tegen, I., Lacis, A. A. and Fung, I. 1996. The influence of mineral aerosols from disturbed soils on the global radiation budget. *Nature* **380**, 419–422.
- Unsworth, M. H. and Monteith, J. L. 1972. Aerosol and solar radiation in Britain. *Q. J. R. Meteorol. Soc.* **98**, 778–797.
- Wang, G., Kong, Q., Ren, L., Gu, Z. and Emilenko, A. 2002. Black carbon aerosol and its variations in the urban atmosphere in Beijing area. *Chinese J. Process Eng.* **2**, 283–288.
- Wei, D. and Qiu, J. 1998. Wideband method to retrieve the imaginary part of complex refractive index of atmospheric aerosols, part I: Theory. *Chinese J. Atmos. Sci.* **22**, 677–685.
- Winchester, J. W., Lu, W., Ren, L., Wang, M., and Maenhaut, W. 1981. Fine and coarse aerosol composition from a rural area in northern China. *Atmos. Environ.* **15**, 933–937.
- Yang, J. and Qiu, J. 2002. A method for estimating precipitable water and effective water vapor content from ground humidity parameters. *Chinese J. Atmos. Sci.* **26**, 81–96.
- Zhang, R., Xu, Y. and Han, Z. 2003. Inorganic chemical composition and source signature of PM<sub>2.5</sub> in Beijing during the ACE-ASIA period. *Chinese Sci. Bull.* **48**, 1002–1005.